Phase Coherent Digital Communications for Wireless Optical Links in Turbid Underwater Environments

Brandon Cochenour, *Member, IEEE,* Linda Mullen, *Senior Member, IEEE,* Alan Laux

Naval Air Systems Command

22347 Cedar Point Rd

Patuxent River, MD 20634

Abstract- **Previous studies by the authors have included a theoretical and experimental investigation of the spatial distribution of an optical signal used for communications in underwater scattering environments. Presented here is an experimental study of how scattering affects the temporally encoded information bearing component of the optical signal. Short range underwater optical links employing BPSK, QPSK, 8-PSK, 16-QAM, and 32-QAM modulation are implemented in a laboratory setting, yielding data rates up to 5Mb/s. The effect of link quality is examined versus water turbidity.**

I. INTRODUCTION

Optical techniques for wireless communication underwater have experienced a recent resurgence in interest from both the scientific and military communities. While acoustic methods have enjoyed the most success in this area, the acoustic carrier is ultimately limited in bandwidth due to frequency dependent absorption, energy spreading, and multi-path reflections [1]. As such, optical methods for wireless undersea communication are becoming an attractive alternative for high speed data links.

Optical links however will lack the range that acoustic systems provide. This is mainly attributed to the absorption and scattering of photons by underwater particulates. Absorption can be minimized through choice of source wavelength, and therefore sources in the blue/green spectral window are used for underwater applications. In turbid ocean or harbor environments, it is likely that scattering of photons will be the dominant source of optical power loss. It is important then to understand not only the spatial properties of scattered light in the ocean, but also how the scattering will affect the temporally encoded information signal.

Previous efforts by the authors have theoretically and experimentally investigated both the spatial properties of scattered optical signals as well as a brief investigation of the time-dependent effects of optical scattering [2]. Presented here is a more thorough experimental investigation of the temporal characteristics of optical communication signals in turbid water environments. Specifically, we investigate several coherent modulation schemes such as phase shift keying (PSK) and quadrature amplitude modulation (QAM). Implementation of these schemes is unique, since most work in underwater optical communications has focused on schemes using optical pulses [3,4]. These pulsed studies focused on baseband modulation formats where the data rate increases with higher pulse repetition rate and shorter pulse widths. This must be achieved while maintaining sufficient pulse-to-pulse amplitude stability and minimizing timing jitter. Development of these sources at wavelengths appropriate for the underwater environment continues to be an active area of research, as is the study of the propagation characteristics of these pulses through scattering media such as turbid ocean water. Similarly, links employing on-off keying (OOK) have been reported, though only for operation in clear deep ocean waters [5].

On the other hand, more efficient phase coherent schemes can be easily implemented with readily available continuous wave laser sources and off the shelf electro optic (EO) modulators. Here, data is encoded onto the optical signal by intensity modulating the laser. This is an attractive option since the data rate can be increased by employing a more complex signaling scheme (M-PSK, M-QAM). Thus, a higher data rate can be achieved while still maintaining a narrow receiver bandwidth. The reader is cautioned that throughout this paper the authors will refer to "coherent" as related to the intensity modulation imposed on the optical carrier. This is not the same as the coherence of the optical signal itself.

The question remains as to how the underwater environment will affect the utility of these coherent schemes. Therefore, the focus of this work is to investigate the effects that scattering will have on an intensity modulated optical signal, and to determine what coherent modulation schemes can be realistically implemented in the challenging underwater environment.

II. EXPERIMENTAL SETUP

An experimental setup was created to test the effect of the water on an encoded optical signal. A block diagram of the laboratory link is given in Fig. 1. A continuous wave green laser (532nm) was intensity modulated at 70MHz by an electro-optic (EO) modulator. The EO modulator was driven by a vector signal generator (VSG) that can be configured to provide BPSK, QPSK, 8-PSK, 16-QAM, and 32-QAM signaling centered on the 70MHz carrier. Therefore, the intensity modulated optical signal can be represented by the following equation:

$$P_T(t) = P_0(1 + M_j(t)\cos(2\pi ft + \phi_j(t)))\qquad(1)$$

where P_0 is the average optical power, f is the modulation frequency (f=70MHz), $M_j(t)$ is the modulation depth of the j-th symbol, and $\phi_j(t)$ is the phase of the j-th symbol.

Report Documentation Page		*Form Approved* *OMB No. 0704-0188*

1. REPORT DATE **SEP 2007**	2. REPORT TYPE	3. DATES COVERED **00-00-2007 to 00-00-2007**

4. TITLE AND SUBTITLE **Phase Coherent Digital Communications for Wireless Optical Links in Turbid Underwater Environments**	5a. CONTRACT NUMBER
	5b. GRANT NUMBER
	5c. PROGRAM ELEMENT NUMBER
6. AUTHOR(S)	5d. PROJECT NUMBER
	5e. TASK NUMBER
	5f. WORK UNIT NUMBER

7. PERFORMING ORGANIZATION NAME(S) AND ADDRESS(ES) **Naval Air Systems Command,22347 Cedar Point Rd,Patuxent River,MD,20634**	8. PERFORMING ORGANIZATION REPORT NUMBER
9. SPONSORING/MONITORING AGENCY NAME(S) AND ADDRESS(ES)	10. SPONSOR/MONITOR'S ACRONYM(S)
	11. SPONSOR/MONITOR'S REPORT NUMBER(S)

12. DISTRIBUTION/AVAILABILITY STATEMENT
Approved for public release; distribution unlimited

13. SUPPLEMENTARY NOTES
See also ADM002047. Presented at the MTS/IEEE Oceans 2007 Conference held in Vancouver, Canada on Sep 29-Oct 4, 2007.

14. ABSTRACT
See Report

15. SUBJECT TERMS

16. SECURITY CLASSIFICATION OF:			17. LIMITATION OF ABSTRACT	18. NUMBER OF PAGES	19a. NAME OF RESPONSIBLE PERSON
a. REPORT **unclassified**	b. ABSTRACT **unclassified**	c. THIS PAGE **unclassified**	**Same as Report (SAR)**	**5**	
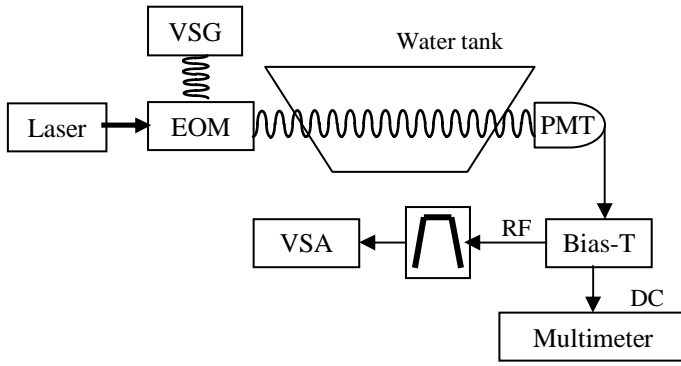
Fig 1. Set-up of the laboratory underwater link

input of the demodulator), which can be measured in several ways. The first approach is to directly compare the transmitted and received sequences. To do this, the vector signal generator was configured to generate a pseudorandom sequence of 2000 symbols. In order to obtain a moderate level of statistics, analysis was performed on over 100,000 symbols, which yields a test set of 50 packets. Symbol error was then calculated by comparing the demodulated packet sequence with the original 2000 symbol sequence.

A second metric for quantifying the effect of water turbidity on link quality is through statistical analysis of the received digital symbols themselves. The modulation error ratio (MER) was chosen in this study for this purpose, and is defined as,

$$MER = \frac{\sum_{j=1} (\tilde{I}_j^2 + \tilde{Q}_j^2)}{\sum_{i=1}^{N} [(I_j - \tilde{I}_j)^2 + (Q_j - \tilde{Q}_j)^2]} \qquad (3)$$

where I_j and Q_j are the real and imaginary components of the j-th received symbol, and $\tilde{I}_j$ and $\tilde{Q}_j$ are the components of the ideal (i.e. - expected) j-th symbol received. In this form, the MER can be thought of a "vectorized" measurement of the signal-to-noise per symbol, with the numerator of (3) representing the average symbol power and the denominator representing the average symbol error power. As such, the MER is an ideal measurement for the VSA hardware and software to make.

The modulation depth is defined as the ratio of the modulated component ($P_{max} - P_{min}$) to the average optical power (P_{ave}) such that,

$$M = \frac{\frac{1}{2}(P_{max} - P_{min})}{\frac{1}{2}(P_{max} + P_{min})} = \frac{\frac{1}{2}(P_{max} - P_{min})}{P_{ave}} \qquad (2)$$

For PSK schemes, $M_j = 1$ and $\phi_j(t)$ varies per symbol, while both the modulation depth and phase will change to represent different symbols in QAM. In all tests, the symbol rate was 1MS/s, providing bit rates of 1Mbps to 5Mbps depending on the chosen modulation scheme.

A small water tank was used as the underwater channel. The tank is 1m x 1m x 3.6m, and has large windows on each end. Maalox antacid, commonly used to simulate scattering in the ocean, was used to change water turbidity [6]. The water was circulated via a pump to maintain a homogeneous water column. The beam attenuation coefficient, $c(\lambda)$, which describes the optical loss due to the cumulative effects of absorption and scattering, was measured at λ=532nm for each Maalox concentration with a transmissometer located in-situ.

At the opposite end of the tank, a photomultiplier tube (PMT) is precisely aligned with the transmitted beam. The PMT has an aperture of 8mm and a field of view of 100 degrees. Such a large field of view was desired to maximize the amount of scattered photons collected by the receiver in order to best determine the impact that multiple scattering may have on the optical link. The received signal is split into the AC and DC components via a bias-T. The DC component was monitored with a multimeter to assure that that the receiver operates within its linear dynamic range, while the AC component is bandpass filtered and processed by a vector signal analyzer (VSA). Custom software written in LabView (National Instruments) performs the necessary demodulation, signal measurement and analysis at the VSA.

The goal of the experiments was to determine the effect of water turbidity on link quality (i.e. – signal-to-noise at the

III. RESULTS

Fig. 2 provides the experimental results of probability of symbol error, P_M, versus MER for each of the five modulation schemes. These measurements were made in clean water (no Maalox added) so that limitations of the modulation scheme and the experimental set up could be analyzed before considering the effects of water turbidity on the optical link. For each modulation scheme, the optical power was reduced until $P_M > 0$ (i.e., an error was detected). The MER and P_M were then calculated for that scenario and for subsequent lower optical power levels until P_M became significant enough ($>10^{-1}$) such that symbol errors would be expected to spoil the MER measurements (i.e. – received symbols compared to the incorrect "ideal" symbol of (3)). The results of Fig. 2 shows that a MER of 30dB insures that all five modulation schemes can be implemented with $P_M > 10^{-5}$.

Of particular interest of course in the underwater scenario is how MER, and therefore P_M, will change as a function of water turbidity. The water clarity may affect link quality in two different ways. First, the amount of light that reaches the receiver is directly dependent on the turbidity of the water channel. Light attenuates exponentially with range according to

$$P_R = P_0 e^{-\delta l} \qquad (4)$$

where P_R is the optical power detected over a certain link range, d, and $\delta = a + kb$ is the water-dependent attenuation coefficient with both absorption (a), and scattering (b) components.
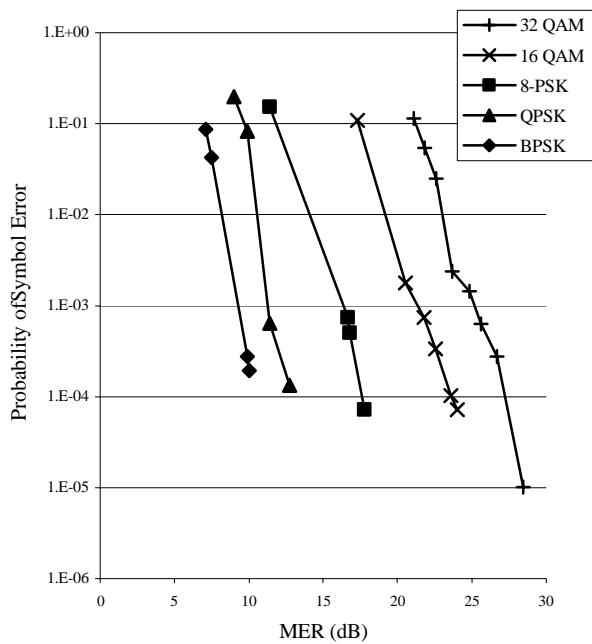
Fig. 2 - Probability of Symbol Error vs MER in clean water over a 3.6m range

It may seem that collecting light that is multiply scattered (k<1) would be beneficial for a communications link. From a purely optical power efficiency point of view, this is true; however we must consider the effect of optical scattering on the time encoded portion of our signal, and not just the average optical intensity. In the setup described here, the 70MHz intensity modulation is coded with the information signal. In turbid waters it is plausible that enough optical scattering events will occur that produce path length differences within the receiver's field of view that are significant relative to the 70MHz wavelength. The result may lead to a decrease in modulation depth beyond what was transmitted, and therefore loss of MER. The net effect may be similar to the multipath reflections that plague acoustic systems

To examine the impact of these two potential forms of loss, experiments were performed at different water clarities. For a given Maalox concentration (and beam attenuation coefficient), the MER was measured at different transmitted optical power levels. To achieve the most accurate MER measurement (i.e. – a symbol signal to noise not spoiled by decision errors), the MER for BPSK signaling is shown in the following data since BPSK will be the most immune to errors.

The results are shown in Fig. 3 where the MER is plotted for different transmitted optical power levels for beam attenuation coefficients ranging from those corresponding to clean, open ocean water (c=0.11/m) to those associated with more turbid harbor scenarios (c=3.0/m). In the low turbidity case of c=0.11/m shown in Fig.3, only -40dBm of optical power was required to achieve a MER of 30dB. However, as water turbidity increases, significantly more transmitted optical power is required since many of the outgoing photons are multiply scattered before reaching the receiver. We see that in the very turbid water case of c=3.0/m, we require ~5dBm of transmitted optical power to achieve the same MER of 30dB. Thus, a 45dB increase in optical power is needed in turbid harbor waters to compensate for the exponentially attenuated optical signal.

Here, k is the fraction of scattered light that is not recovered by the receiver. Therefore, the range of the attenuation coefficient (δ) is $c < \delta < a$ depending on the receiver acceptance angle. For scenarios dominated by non-scattered light, $k \approx 1$ and therefore $\delta \approx c$.

The second way that the water clarity may affect an optical communications link is by inducing multiple optical scattering.
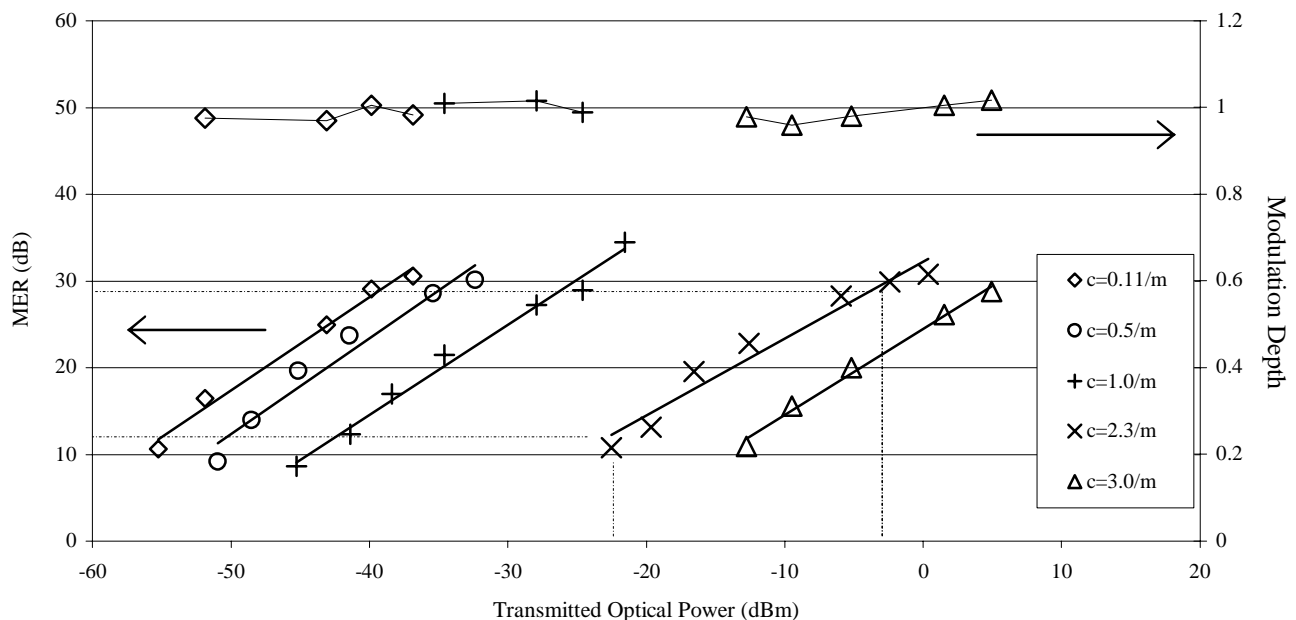

Fig 3. MER (left axis) and modulation depth (right axis) vs. transmitted optical power for various water turbidities.

If the received photons for any turbidity are mostly non-scattered, then by (4), the amount of additional transmitted optical power necessary to achieve the same received optical power (and hence same MER) between two water turbidities is given as,

$$10\log\frac{P_{0,2}}{P_{0,1}} = 10\log\frac{e^{-c_1 d}}{e^{-c_2 d}} \qquad (5)$$

where $P_{0,1}$ and $P_{0,2}$ are the transmitted optical powers at water turbidities c_1 and c_2 respectively. Substituting the attenuation coefficients from above (i.e., $c_1 = 0.11/m$ and $c_2 = 3.0/m$) into (5), we find the power ratio to be ~45dB, which suggests that the received signal is dominated by non-scattered (or very minimally scattered) light.

To further confirm this, we examine the modulation depth as a function of water turbidity. Results are summarized in Fig. 3 where modulation depths for three water turbidities are plotted on the right axis. Since we are mainly interested in potential modulation loss of the carrier signal, we focus on the PSK modulation schemes where the modulation depth $M_i(t) = 1$ for all symbols and examine for any deviation from unity. Note that no loss of modulation depth has occurred, suggesting that at this range and carrier frequency, multiple scattering has not produced significant enough path length differences to degrade the modulated sub-carrier. Also note that this may have been predicted by examination of the slopes of the curves in Fig. 3. The similarity in slope between data sets suggests that for each water turbidity, there is a linear relationship between MER and transmitted optical power. Had modulation loss occurred at higher water turbidities the relationship between MER and transmitted optical power may have had a more complex association. Further study is needed to determine exactly what this relationship may be.

It is now obvious that we can use Figs. 2 and 3 as a graphical method for determining link budgets in turbid waters. For example, consider the case where an underwater link is needed in turbid waters with a $c=2.3/m$. A laser transmitter is available that is capable of providing -2.4dBm of optical power. According to Fig. 3, over a range of 3.6m (the test tank), a MER of ~30dB will be achieved at the receiver. By use of Fig. 2, we see that 30dB of MER will provide symbol error performance better than ~10^{-5} for all modulation formats. This is illustrated in Fig. 4, which shows the constellation diagrams for each of the five modulation schemes, along with the MER and P_M for this condition.

Note that in fig. 4 that for 16- and 32-QAM, the MER is slightly lower, and the P_M of 32-QAM is higher than predicted. This is not due to the environment, but rather the hardware used in the experiment. The vector signal generator will output the same average power for both the PSK and QAM signal sets. However, because QAM symbols employ both phase and amplitude changes, symbols at the edge of the constellation will have a higher peak power than PSK symbols. It was discovered that these higher peak powers caused the EO modulator to be overdriven, resulting in distortion of the modulated optical signal. For this reason, the average power delivered to the EO modulator was reduced for the QAM schemes, which resulted in an inherently lower MER, typically 3-5dB less than PSK signaling for the same water turbidity and optical power.

Fig. 5 shows the results when operating at an optical power of -22.52dBm in the same water turbidity. The lower transmitted power results in a MER of ~10dB as shown by Fig. 3. Using Fig. 2, we can predict that only BPSK and QPSK will be successful in this regime. The constellation diagrams of fig. 5 confirm that this is true. For 8-PSK, 16-QAM, and 32-QAM, there was not enough MER to close the link.
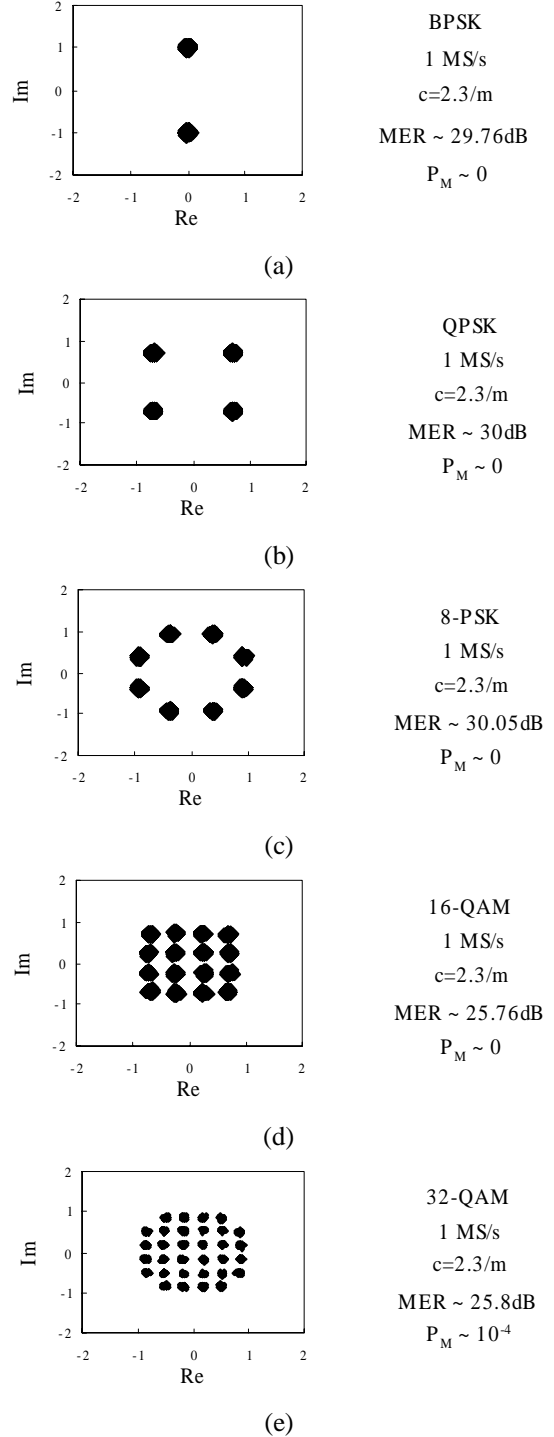

BPSK
1 MS/s
c=2.3/m
MER ~ 29.76dB
$P_M \sim 0$

(a)

QPSK
1 MS/s
c=2.3/m
MER ~ 30dB
$P_M \sim 0$

(b)

8-PSK
1 MS/s
c=2.3/m
MER ~ 30.05dB
$P_M \sim 0$

(c)

16-QAM
1 MS/s
c=2.3/m
MER ~ 25.76dB
$P_M \sim 0$

(d)

32-QAM
1 MS/s
c=2.3/m
MER ~ 25.8dB
$P_M \sim 10^{-4}$

(e)

Fig 4. Constellation diagrams for (a) BPSK, (b) QPSK, (c) 8-PSK, (d) 16-QAM, and (e) 32-QAM in c=2.3/m water. The transmitted optical power is -2.4dBm and the symbol rate is 1×10^{6} symbols/sec

BPSK

1 MS/s

c=2.3/m

MER ~ 10.42dB

P_M ~ 0

(a)

QPSK

1 MS/s

c=2.3/m

MER ~ 10.86dB

P_M ~ 10^{-3}
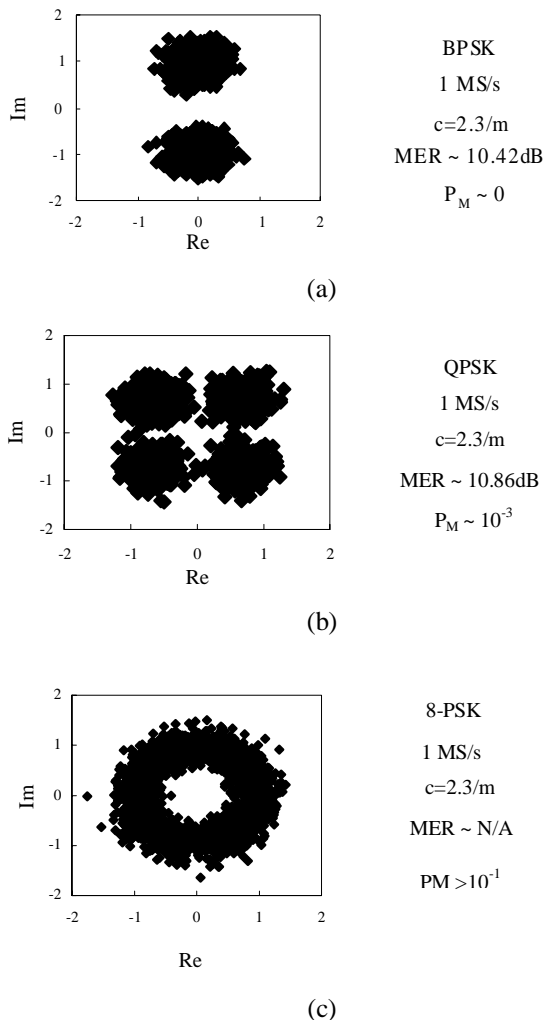
(b)

8-PSK

1 MS/s

c=2.3/m

MER ~ N/A

PM > 10^{-1}

(c)

Fig. 5. Constellation diagrams for (a) BPSK, (b) QPSK, and (c) 8-PSK in c=2.3/m water. The transmitted optical power is -22.52dBm and the symbol rate is 1×10^6 symbols/sec. As shown, at this power level and turbidity, only the BPSK and QPSK links are able to be closed. 16- and 32- QAM not shown.

IV. CONCLUSIONS

Experiments were conducted to study the effects of the underwater environment on several phase coherent modulation formats. Relationships between source power, water turbidity, and signal to noise were shown for a short range laboratory link. Scattering was shown to have little effect on the information bearing component of the optical signal, as no modulation depth was lost, even in the most turbid waters. For sufficient optical powers, 5 Mbps links were closed using 32-QAM signaling. Under these same conditions, data rates approaching 50 Mbps or higher could be achievable with small changes in the VSG/VSA hardware and software.

It should be noted however that link range will play a large part in determining the performance of phase coherent schemes underwater. For instance, given a single water turbidity the intensity of an optical signal decreases exponentially versus link range. Furthermore the modulation depth of the received signal will be not only a function of range, but modulation frequency and water turbidity as well. More study is required to understand these relationships at physical ranges longer than those provided by the test tank. Regardless, we posit that for modulation frequencies comparable to those studied here, it would require a significantly larger physical path length before multipath effects may occur.

In this study, the transmitter and receiver were precisely aligned such that the receiver recovered both non-scattered and scattered photons. In practice, there will likely be some pointing mismatch between transmitter and receiver which requires additional consideration. Under multiple scattering, the directionality characteristic of the optical signal approaches that of a diffuse source as photons are scattered away from the main beam. While this spatial spreading may help ease system pointing and tracking requirements, it decreases the received signal since the majority of photons are scattered and do not get captured. From the temporal perspective, when the transmitter and receiver exhibit some pointing mismatch, a loss of modulation depth may occur since the photons that are captured have been multiply scattered and may potentially have accumulated sufficient path length differences. Prior study of modulation depth for moderate transmitter/receiver pointing accuracies for extremely turbid waters (c=~20/m) in the same water tank used in this study have been made in [2]. While there were no significant degradations to the modulated signal, further study must be done at longer path lengths and more sever transmitter/receiver pointing mismatches. Experiments at these longer ranges will provide greater insight as to the limitation that the environment will have on the modulated signal. Preliminary results however suggest that for short ranges (<100m), phase coherent links are a viable option for high speed data transfer underwater.

REFERENCES

[1] M. Stojanovic, "Recent advances in high speed underwater acoustic channels", *IEEE Journal of Oceanic Engineering*, VOL. 21, NO. 2, April 1996.
[2] B. Cochenour, T. Curran, L. Mullen, A.Laux, "Effects of multiple scattering on the implementation of an underwater wireless optical communications link," *Proc. Oceans 2006*, pp. 1-6. Sept, 2006
[3] J.B. Snow, et. al., "Underwater propagation of high data rate laser communications pulses," *SPIE Ocean Optics XI*, vol. 1750. 1992.
[4] M. Chen, S. Zhou, T. Li. "The implementation of PPM in underwater laser communications system," *International Conference on Communications, Circuits and Systems Proceedings,* Volume 3, 25-28 pp. 1901 – 1903. June 2006.
[5] N. Farr, A. Chave, L. Freitag, J. Preisig, S. White, D. Yoerger, P. Titterton, "Optical modem technology for seafloor observatories," *Proc. OCEANS 2005.* pp 928 - 934 Vol. 1. 2005.
[6] A. Laux, R. Billmers, L. Mullen, B. Concannon, J. Davis, J. Prentice, and V. Contarino, "The a,b,c's of oceanographic lidar predictions: a significant step towards closing the loop between theory and experiment", *Journal of Modern Optics*, VOL. 49, NO. 3/4, 439-451. 2002.